Title	A floating box-type breakwater with slotted barriers
Author(s)	Huang, Zhenhua; He, Fang; Zhang, Wenbin
Citation	Huang, Z., He, F., & Zhang, W. (2014). A floating box-type breakwater with slotted barriers. Journal of Hydraulic Research, in press.
Date	2014
URL	http://hdl.handle.net/10220/19857
Rights	© 2014 International Association for Hydro-Environment Engineering and Research. This is the author created version of a work that has been peer reviewed and accepted for publication by Journal of Hydraulic Research, International Association for Hydro-Environment Engineering and Research. It incorporates referee’s comments but changes resulting from the publishing process, such as copyediting, structural formatting, may not be reflected in this document. The published version is available at: [DOI: http://dx.doi.org/10.1080/00221686.2014.888690].

PROOF COVER SHEET

Author(s): Zhenhua Huang

Article title: A floating box-type breakwater with slotted barriers

Article no: TJHR888690

Enclosures: 1) Query sheet

2) Article proofs

Dear Author,

1. Please check these proofs carefully. It is the responsibility of the corresponding author to check these and approve or amend them. A second proof is not normally provided. Taylor & Francis cannot be held responsible for uncorrected errors, even if introduced during the production process. Once your corrections have been added to the article, it will be considered ready for publication.

Please limit changes at this stage to the correction of errors. You should not make insignificant changes, improve prose style, add new material, or delete existing material at this stage. Making a large number of small, non-essential corrections can lead to errors being introduced. We therefore reserve the right not to make such corrections.

For detailed guidance on how to check your proofs, please see
http://journalauthors.tandf.co.uk/production/checkingproofs.asp.

---

2. Please review the table of contributors below and confirm that the first and last names are structured correctly and that the authors are listed in the correct order of contribution. This check is to ensure that your name will appear correctly online and when the article is indexed.

Sequence	Prefix	Given name(s)	Surname	Suffix
1.		Zhenhua	Huang	
2.		Fang	He	
3.		Wenbin	Zhang	

Queries are marked in the margins of the proofs.

AUTHOR QUERIES

General query: You have warranted that you have secured the necessary written permission from the appropriate copyright owner for the reproduction of any text, illustration, or other material in your article. (Please see http://journalauthors.tandf.co.uk/preparation/permission.asp.) Please check that any required acknowledgements have been included to reflect this.

QUERY NO.	**QUERY DETAILS**
AQ1	Please check all equations, special characters, symbols and figures to ensure they adhere to journal style and are correct and consistent throughout the article. Please note, symbols and special characters in figures should be consistent with those in the text.
AQ2	Please spell out “CFD” in full at first mention.
AQ3	Please check if the given issue number is correct.
AQ4	Please provide missing article title for the “Mavrakos (1992)” references list entry.

How to make corrections to your proofs using Adobe Acrobat

Taylor & Francis now offer you a choice of options to help you make corrections to your proofs. Your PDF proof file has been enabled so that you can edit the proof directly using Adobe Acrobat. This is the simplest and best way for you to ensure that your corrections will be incorporated. If you wish to do this, please follow these instructions:

1. Save the file to your hard disk.

2. Check which version of Adobe Acrobat you have on your computer. You can do this by clicking on the "Help" tab, and then "About."

If Adobe Reader is not installed, you can get the latest version free from http://get.adobe.com/reader/.

- If you have Adobe Reader 8 (or a later version), go to "Tools"/"Comments & Markup"/ "Show Comments & Markup."
- If you have Acrobat Professional 7, go to "Tools"/ "Commenting"/"Show Commenting Toolbar."

3. Click "Text Edits." You can then select any text and delete it, replace it, or insert new text as you need to. If you need to include new sections of text, it is also possible to add a comment to the proofs. To do this, use the Sticky Note tool in the task bar. Please also see our FAQs here: http://journalauthors.tandf.co.uk/production/index.asp.

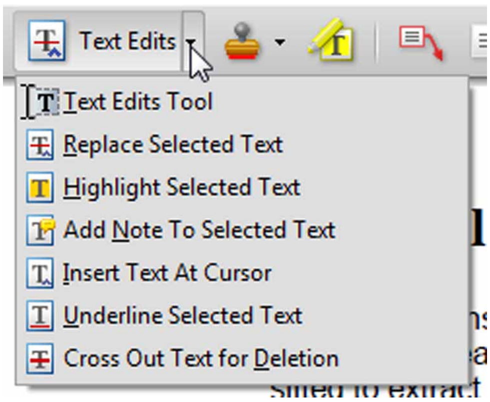

4. Make sure that you save the file when you close the document before uploading it to CATS using the "Upload File" button on the online correction form. A full list of the comments and edits you have made can be viewed by clicking on the "Comments" tab in the bottom left-hand corner of the PDF.

If you prefer, you can make your corrections using the CATS online correction form.

Journal of Hydraulic Research Vol. 00, No. 0 (2014), pp. 1–8
http://dx.doi.org/10.1080/00221686.2014.888690

Technical note

A floating box-type breakwater with slotted barriers

ZHENHUA HUANG, Assistant Professor, *School of Civil and Environmental Engineering, Nanyang Technological University, 50 Nanyang Avenue, Singapore 639651, Singapore; School of Ocean and Earth Science and Technology, University of Hawaii at Manoa, Honolulu, HI 96822, USA*
Email: zhenhua@hawaii.edu, zhhuang@ntu.edu.sg (author for correspondence)

FANG HE, PhD Student, *School of Civil and Environmental Engineering, Nanyang Technological University, 50 Nanyang Avenue, Singapore 639651, Singapore*
Email: hefa0003@e.ntu.edu.sg

WENBIN ZHANG, Project Officer, *School of Civil and Environmental Engineering, Nanyang Technological University, 50 Nanyang Avenue, Singapore 639651, Singapore*
Email: zhangwenbin0412@hotmail.com

ABSTRACT
Floating box-type breakwaters are frequently used for small harbours and marinas. This paper reports a comparative experimental study of the performance of a rectangular floating breakwater with and without slotted barriers. Experimental results showed that the slotted barriers attached to the bottom of a floating box-type breakwater could improve the transmission performance without increasing both the heave and surge motion responses. It was also found that the slotted barriers could reduce the pitch motion responses for shorter waves and increase the pitch motion responses for longer waves.

Keywords: Coastal engineering; coastal structures; floating breakwater; gravity waves; laboratory studies; ocean engineering; wave–structure interactions

1 Introduction

Q1 Breakwaters are widely used to reduce wave energy either inside a harbour or impacting on coast-lines and coastal structures (Koutandos *et al.* 2005, Wang and Sun 2010, Huang *et al.* 2011, Tomasicchio and D'Alessandro 2013). Rubble mound breakwaters and vertical wall breakwaters are two traditional forms of bottom-sitting breakwaters. However, in the places where the water depth is relatively deep, traditional bottom-sitting breakwaters are not only very expensive to build, but also environmentally unfriendly since they may block the water and sediment exchange between the harbour and the ocean. As alternatives to traditional bottom-sitting breakwaters, floating breakwaters have received much attention recently; this is because floating breakwaters can be deployed with flexibility and mobility, can adjust their elevation with variable water levels, allow water and sediment exchange underneath, and are less dependent on bottom soil conditions. However, floating breakwaters are known to be less efficient for longer waves. Therefore, improving the performance of floating breakwaters for longer waves is of practical interests. For an early review of designs and applications of various floating breakwaters, please refer to McCartney (1985).

A simple design of floating breakwater is a partially immersed rectangular box (Drimer *et al.* 1992, Sannasiraj *et al.* 1998). For a fixed box-type breakwater with a given draught, the ratio of the breakwater width to wave length is the most important design parameter (Black *et al.* 1971, Williams 1988); for a floating box-type breakwater, the motion responses of the breakwater to waves can affect the loads in the mooring lines and may also affect the transmission performance of the breakwater. For a given floating breakwater, the transmission performance of the floating breakwater is usually poor when the ratio of the breakwater width to wave length is not large enough.

Many novel designs have been proposed to reduce wave transmission for this type of breakwaters: for example, attaching a

Revision received 27 March 2013/Currently open for discussion.

ISSN 0022-1686 print/ISSN 1814-2079 online
http://www.tandfonline.com

row of pipes to the bottom of a floating trapezoidal shape breakwater (Mani 1991); making the body of the floating box-type breakwater porous (Wang and Sun 2010); extending two vertical thin plates down from both sides of a floating box-type breakwater (Peña *et al.* 2011, Ruol *et al.* 2013); adding a single porous plate at the front part of a heaving box-type breakwater (Koutandos *et al.* 2005); attaching pneumatic chambers on both sides of a floating box-type breakwater (He *et al.* 2012, 2013). Slotted barriers can be very effective in reducing wave energy over a relatively wide range of wave periods (Huang *et al.* 2011). In the present study, we propose a new design of floating box-type breakwater with three rows of slotted barriers attached to its bottom.

In this study, the hydrodynamic performance of a floating box-type breakwater with slotted barriers attached to its bottom will be investigated experimentally and compared with that of the same floating box-type breakwater without slotted barriers. The objective of this comparative study is to demonstrate that attaching slotted barriers to a floating breakwater can reduce wave transmission without significantly increasing motion responses.

2 Experimental setup

The experiments were conducted in a wave flume located in the Hydraulics Laboratory at Nanyang Technological University, Singapore. The wave flume is 45 m in total length, 1.55 m in width and 1.5 m in depth. At one end of the flume, a piston-type wave generator is equipped with an active wave absorption control system to reduce the wave reflection from the wave paddle. At the other end, there is a beach covered with several porous mats to minimize wave reflection.

2.1 *The breakwater models and mooring system*

The box-type breakwater model used in this study was 1.42 m in length, 0.75 m in width and 0.40 m in height. For the convenience of fabrication and installation, the model was built as two separate but identical parts that can be bolted together. Referring to Fig. 1, three rows of slotted barriers, made of hollow square aluminium bars, were attached to the bottom of the breakwater. Each aluminium bar had a square cross-section of 9 mm × 9 mm and the length of each bar was 250 mm. The centre-to-centre distance between two bars was 15 mm (i.e. the gap was 6 mm), resulting in a value of 0.4 for the porosity of the slotted barriers. The distance between two adjacent rows was kept at 305 mm. The box-type breakwater was made of 10-mm thick Perspex sheets and a specified draught was achieved by adding ballast weight inside the model (steel and Perspex plates). The total weight of the slotted barriers was small compared with the weight of the model itself. After the installation of the three rows of slotted barriers, we adjusted ballast weight so the two models had the same weight. Due to the additional buoyant forces associated with the hollow aluminium bars, the draught for the model with slotted barriers was slightly smaller (4 mm smaller) than that without: the draught was 0.213 m for the model with the slotted barriers, and 0.217 m for the model without the slotted barriers. The detailed information of the two models is summarized in Table 1 for reference.

In the present experiment, the water depth was fixed at $h = 0.9$ m and the model was slack-moored at 25 m away from the wave generator. Three sets of mooring lines were installed on each side of the model, and each mooring line was fastened to a concrete anchor. The touchdown point of each mooring line was about 1 m away from the model centreline and the anchor point was 3 m away from the model centreline. The stainless-steel mooring lines had a length of 3.0 m each, and the line density

Table 1 Details of the models examined in the experiments

Model	Length (mm)	Width (mm)	Height (mm)	Draught (mm)	Mass (kg)	Moment of inertia (kg m^2)	CG (mm)
Model 1	1420	750	410	217	231	14.5	88.5
Model 2	1420	750	410	213	231	16.3	80.4

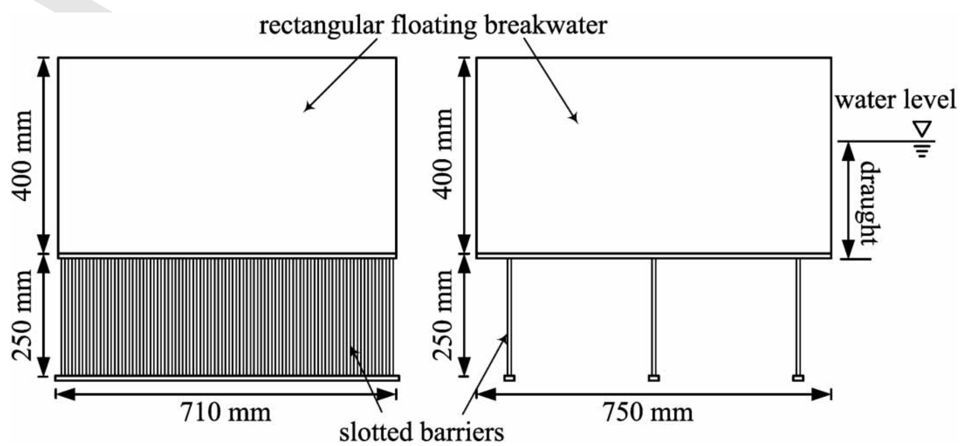

Figure 1 Details of the floating breakwater with slotted barriers. Left: front view showing the arrangement of the aluminium bars in a row; right: side view showing three rows of slotted barrier

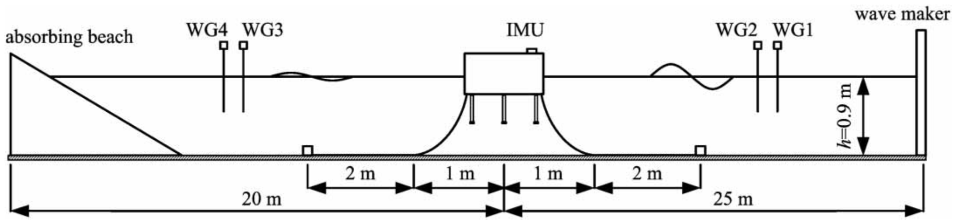

Figure 2 A sketch of experimental setup

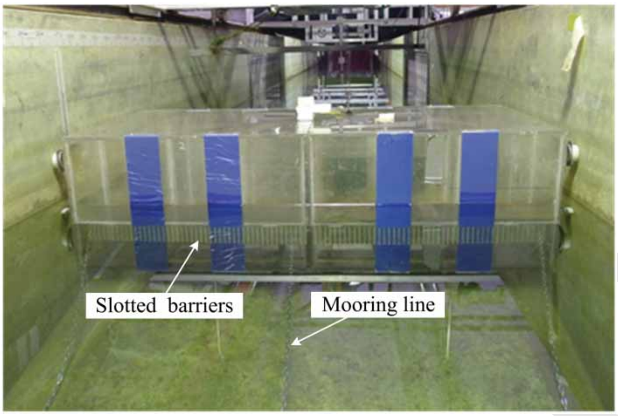

Colour online, B/W in print

Figure 3 A view of the model with slotted barriers installed in the wave flume

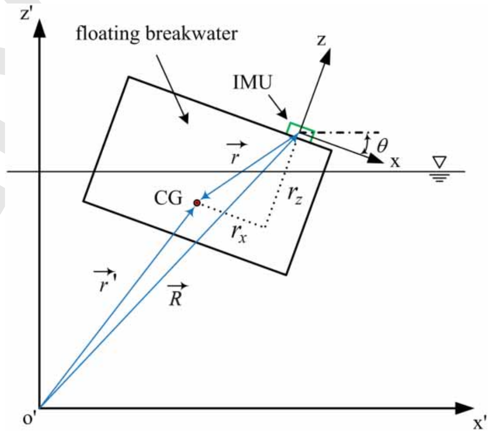

Colour online, B/W in print

Figure 4 Definition sketch of the two coordinate systems for calculating RAOs

was 0.155 kg m^{-1}. The mooring-line scope (defined as the ratio of the length of a mooring line to the water depth) was 3.33 in this study. The design of the mooring system considered the typical adopted values for the touchdown point, the anchor point, and the mooring-line scope (Mavrakos 1992, Faltinsen 1993). Figure 2 shows the experimental setup, where both the touchdown point and anchor point are also labelled. A view of the breakwater with slotted barriers is shown in Fig. 3.

2.2 *Data collection and analysis*

Four resistance-type wave gauges, each of which had a resolution of 0.1 mm, were used in the experiment to measure surface elevations: two in the seaside and the other two in the leeside of the floating breakwater. The distances between the wave gauges were chosen according to the range suggested by Goda and Suzuki (1976) for performing a two-point wave separation analysis. The amplitudes of the incident waves (A_i), the reflected waves (A_r), the transmitted waves (A_t), and the waves reflected from the beach (A_{rb}) can be obtained by a wave separation analysis. We define the reflection coefficient C_r as A_r/A_i and the transmission coefficient C_t as A_t/A_i. Due to the motion of the breakwater, C_r and C_t include contributions from both scattering waves and radiated waves.

The motion responses of the floating breakwater to waves were recorded by an inertia measurement unit (IMU), which was mounted at one corner on the top plate of the model. The sampling frequency of the IMU was 200 Hz in this study. The IMU measures the accelerations of the three translational motions and angular velocities of the three rotational motions. In this study, only three degree-of-freedom responses (surge, heave and pitch) were allowed.

For small amplitude waves, the motion responses of the breakwater to monochromatic waves can be well described by sinusoidal functions. Referring to Fig. 4, two coordinate systems are needed to determine the response amplitude operators (RAOs): an earth-fixed coordinate system by (x', z'), and an IMU-fixed coordinate system by $(x,\ z)$. The linear translational accelerations $(a_{x'}(t), a_{z'}(t))$ of the centre of gravity (CG) in the earth-fixed coordinate system can be determined by the following relationships:

$$a_{x'}(t) \approx A_x(t) + \ddot{\theta}(t) r_z \equiv \hat{a}_{x'} \sin(\omega t + \phi_{a_{x'}}) \tag{1}$$

$$a_{z'}(t) \approx A_z(t) - \ddot{\theta}(t) r_x \equiv \hat{a}_{z'} \sin(\omega t + \phi_{a_{z'}}) \tag{2}$$

where $A_x(t)$, $A_z(t)$ and $\dot{\theta}(t)$ are, respectively, the translational accelerations and angular velocity measured by the IMU; ω is the angular frequency of incident waves; (r_x, r_z) are the coordinates of the CG in the IMU-fixed coordinate system, as shown in Fig. 4; the angular acceleration $\ddot{\theta}$ is derived from the time series of $\dot{\theta}$ recorded by the IMU under the assumption that $\dot{\theta}$ is a sinusoidal function. In Eqs. (1) and (2), $(\hat{a}_{x'}, \hat{a}_{z'})$ are the amplitudes of the heave and surge accelerations; $(\phi_{a_{x'}}, \phi_{a_{z'}})$ are the phases, which are immaterial in the analysis. From Eqs. (1) and (2), the amplitudes of the heave and surge responses can be obtained by

$$A_{surge} = \frac{\hat{a}_{x'}}{\omega^2}, \quad A_{heave} = \frac{\hat{a}_{z'}}{\omega^2} \tag{3}$$

The rotational responses in the earth-fixed coordinate system are the same as those measured by the IMU, and the amplitude of the pitch angular-velocity ($\hat{\dot{\theta}}$) can be obtained by a fitting procedure. With A_{surge}, A_{heave} and $\hat{\dot{\theta}}$ being known, the surge, heave and pitch RAOs are defined, respectively, by

$$RAO_{surge} = \frac{A_{surge}}{A_i}, \quad RAO_{heave} = \frac{A_{heave}}{A_i}, \quad RAO_{pitch} = \frac{\hat{\dot{\theta}}}{\omega A_i} \tag{4}$$

2.3 *Possible important control parameters*

The characteristics of wave scattering by the floating structure are mainly controlled by the relative width of the breakwater W/L (Drimer *et al.* 1992); therefore, W/L is one important parameter affecting the transmission performance. It is known that, for a fixed slotted barrier, energy loss is due to the work done by the drag force acting on the slotted barrier; as a result, larger wave heights tend to produce smaller transmission coefficients and slightly larger reflection coefficients for a fixed wave period (Huang 2007). The drag force is quadratically related to the local wave velocity through a drag coefficient. For waves past a fixed vertical cylinder, the drag coefficient varies with the Keulegan–Carpenter number (KC $= U_mT/d$, where U_m is the velocity amplitude and d is the dimension of the cylinder, which is 9 mm in the present study) as well as Reynolds number (R $= U_md/\upsilon$, where υ is the kinematic viscosity of water) (Sarpkaya and Isaacson 1981, Sawaragi 1995, Aristodemo *et al.* 2011). According to Mei *et al.* (2005), the KC number is directly related to A_i/d, where A_i is the amplitude of incoming waves. Therefore, A_i/d can be another important parameter affecting the transmission performance.

Experimental studies on effects of mooring system and wave steepness on floating breakwaters can be found in the literature. For a floating breakwater with a slack-mooring system, the mooring system is used mainly for station-keeping of the floating structure. For a slack-mooring system, its stiffness coefficients for the motion responses are relatively small, and the mooring-line forces in the slack-mooring lines are usually weak. Sannasiraj *et al.* (1998) investigated the performance of a floating breakwater for three slack-mooring configurations; they found that the mooring configurations examined did not significantly affect the wave transmission, and that the moorings at either water level or the bottom of the floating breakwater yielded significantly lesser mooring forces than those with a crossed mooring configuration. Vijayakrishna Rapaka *et al.* (2004) examined three scopes of a slack mooring system for three wave heights. They found that increasing the mooring-line scope from 4 to 6 only slightly reduced the heave RAOs for waves of intermediate frequencies without causing significant changes in both surge and pitch RAOs; they also found that increasing wave height from 0.05 to 0.1 m in a water depth of 1 m only slightly reduced the RAOs of surge, heave and pitch modes for longer waves.

Table 2 Experimental conditions

Parameters	Ranges
Water depth (h)	0.9 m
Wave period (T)	1.1–1.7 s at 0.1 s interval
Wave length (L)	1.88–4.00 m
Wave height (H_i)	0.04 m for all wave periods; 0.02, 0.03, 0.05, 0.06 m for 1.3, 1.4, 1.5 s
A_i/d	1.132, 1.753, 2.295, 2.914, 3.414
Relative width (W/L)	0.187, 0.206, 0.228, 0.256, 0.292, 0.338, 0.399
Wave steepness (H_i/L)	0.01–0.023
Ursell number (U $= H_iL^2/h^3$)	0.18–0.89

2.4 *Test conditions*

Since previous experimental studies have shown that the transmission coefficient of a floating breakwater is weakly dependent on wave steepness, but strongly dependent on the ratio of the breakwater width to wave length (Sannasiraj *et al.* 1998), the present study focused on effects of two most important parameters: W/L and A_i/d. Two sets of tests were carried out in this study. In the first set of tests, we first compared the two breakwaters for various W/L with a fixed value of A_i/d; this was achieved by varying wave period from 1.1 to 1.7 s at 0.1-second intervals while keeping the target wave height at $H_i = 0.04$ m for all wave periods. In the second set of tests, we studied the breakwater with slotted barriers for various A_i/d with a fixed value of W/L; this was achieved by varying the target wave height from 0.02 to 0.06 m at 0.01-meter intervals for a fixed wave period. We selected three wave periods to study the influences of A_i/d: T=1.3, 1.4 and 1.5 s. The reason we chose these three periods was because the transmission coefficient at $T = 1.3$ s was the smallest for $H_i = 0.04$ m according to the results of the first set of tests. Details of the experimental conditions are summarized in Table 2 for reference.

The maximum wave steepness used in the present study was less than 0.023 and the target waves can be classified as weakly-nonlinear waves according to Le Mehaute (1976). The Ursell number (U $= H_iL^2/h^3$) in our experiments ranged from 0.19 to 0.89, indicating that the nonlinearity of the waves used in the tests was weak. Possible effects of mooring scopes, steep waves and irregular waves are outside the scope of the present study.

3 Results and discussion

Experimental results are presented here to demonstrate the effects of the slotted barriers on wave transmission and reflection as well as motion responses. We first present the results obtained with a fixed A_i/d for various values of W/L, and then the results obtained with a fixed W/L for various values of A_i/d.

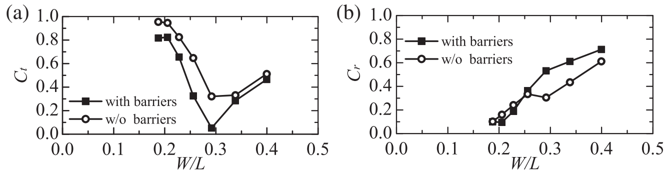

Figure 5 Effects of the slotted barriers on the (a) transmission coefficients and (b) reflection coefficients

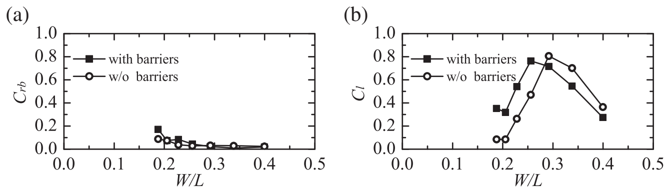

Figure 6 The measured (a) beach-reflection coefficients and (b) energy-loss coefficients

3.1 *Comparison of the two breakwater models: effects of W/L*

Transmission and reflection coefficients

Figure 5 shows the effects of the slotted barriers on the measured transmission and reflection coefficients.

In the absence of the slotted barriers, the smallest transmission coefficient was about 0.32, which occurred at $W/L \approx 0.29$. The slotted barriers reduced the transmission coefficients over the entire range of the tested wave periods, and a minimum transmission coefficient as low as 0.05 occurred at $W/L \approx 0.29$. The slotted barriers also increased the reflection coefficients for shorter waves (i.e. larger values of W/L), but did not significantly affect the reflection coefficients for longer waves (i.e. smaller values of W/L). Unlike a fixed, suspended box-type breakwater, for which transmission coefficient decreases with increasing W/L, a floating breakwater can generate radiated waves and the waves measured in both sides of the breakwater include both the scattered and radiated waves. The phase difference between the scattered waves and radiated waves affects the measured transmission and reflection coefficients (Drimer *et al.* 1992).

Energy-loss coefficient

According to conservation of wave energy, an energy-loss coefficient C_l can be defined using the following equation:

$$C_r^2 + C_t^2 + C_l = 1 + C_{rb}^2 \tag{5}$$

where C_{rb} is the reflection coefficient of the absorbing beach.

The measured C_{rb} and C_l are shown in Fig. 6, which shows that the values of C_{rb}^2 are less than 3% in all tests. The slotted barriers could enhance the loss of wave energy to turbulence only for waves longer than $W/L = 0.29$; on the contrary, the slotted barriers reduced energy loss for waves shorter than $W/L = 0.29$. The maximum energy-loss coefficients for both models are almost the same, indicating that the energy loss caused by the slotted barriers is less than that by the vortex shedding at the sharp edges of the breakwater models. The slotted barriers caused the maximum energy-loss coefficient to occur at a slightly smaller value of W/L, which can be explained partly by the effects of the slotted barriers on pitch motion, as explained later.

Motion responses

Figure 7 shows the effects of the slotted barriers on the motion responses. The slotted barriers had significant effects on both the surge and pitch RAOs, but negligible effects on the heave RAOs.

Since the wave force acting on the slotted barriers is perpendicular to the slotted barriers, and since the two floating breakwater models have almost the same draughts, the installation of the slotted barriers does not significantly affect the static heave-exciting loads (i.e. the buoyancy and the mooring force when the breakwater is in still water). As a result, the installation of the slotted barriers did not significantly affect both the natural period and RAOs of the heave response, as shown in Fig. 7; the slightly-reduced heave RAOs are due partly to the weak coupling between the motion responses.

Referring to Fig. 7, for both models, the surge RAOs are larger for longer waves and smaller for shorter waves. An intuitive explanation is provided below. For a floating breakwater, wave reflection and surge RAOs are related. For shorter waves, the heavy breakwater does not have enough time to respond to waves, leading to smaller surge RAOs and larger reflection coefficients; for longer waves, the breakwater has enough time to adjust itself so that it can travel long distances with waves, leading to larger surge RAOs and smaller reflection coefficients. However, because of the large inertia of the breakwater, there is always a phase difference between the surge response and the wave motion.

The slotted barriers reduced surge RAOs for longer waves ($W/L < 0.30$), but increased the surge RAOs for shorter waves ($W/L > 0.30$). To understand this, we first note that the following two effects of the slotted barriers. (1) Part of the water between the slotted barriers has to move with the breakwater; the total mass of the system is virtually increased for surge motion, which turns to reduce the surge RAOs. (2) A blockage effect introduced by the slotted barriers (i.e. the slotted barriers can effectively block the wave motion underneath the breakwater) may increase the scattering force for surge motion, which turns to increase both the surge RAOs and reflection coefficients. For longer waves, the breakwater may travel long distances with waves, and thus the blockage effect is weak (as indicated by a small reflection coefficient) and the "virtual mass" effect prevails, leading to a reduction in surge RAOs by the slotted barriers; for shorter waves, the breakwater does not have enough time to respond to wave motion, thus the blockage effects prevails (as indicated by a large reflection coefficient), leading to a slight increase in surge RAOs.

For the pitch motion, the slotted barriers significantly reduced pitch RAOs for shorter waves, but significantly increased the pitch RAOs for waves longer than $W/L = 0.25$. Note that the slotted barriers slightly increased the natural period of the pitch response; this is partly because the slotted barriers increased the moment of inertia by 12.4%. A comparison between Figs. 6 and 7 reveals that both the maximum energy loss and the maximum pitch RAO occur at $W/L = 0.29$ for the breakwater without slotted barriers, indicating that the resonant pitch response helps dissipate more energy through vortex shedding at the sharp edges of the floating breakwaters.

We remark that, since the mooring-line force is affected mainly by the surge and heave motions, it is not expected that a moderate increase in the pitch RAOs will significantly increase the mooring-line force.

Discussion on energy-loss and transmission coefficients

For a floating breakwater without slotted barriers, factors that may have contributed to the minimum transmission coefficient include the wave scattering by the floating breakwater, the phase differences between the scattered waves and the radiated waves, and the energy loss due to vortex shedding at the sharp edges of the breakwater. Our slack-mooring system only provides slight restrictions on the motion responses, thus our floating breakwater can be approximately regarded as a freely-floating one. For a freely-floating breakwater in an ideal fluid, a small transmission coefficient may occur when the phase of the radiated waves is approximately opposite to the phase of the scattered waves (see Fig. 2 in Drimer *et al.* 1992). For our breakwater without slotted barriers, both the maximum energy loss and minimum wave transmission occurred at $W/L \approx 0.29$ (Figs. 5 and 6), suggesting that the energy loss due to vortex shedding contributed significantly to the minimum transmission coefficient observed in our experiments. The energy loss depends on the relative velocity between the surrounding water and the moving breakwater at the lower edge of the breakwater. Our results show that the maximum energy loss can be significantly affected by the pitch RAOs, as shown by the following crude order-of-magnitude analysis. The relative velocity is controlled by wave scattering, wave radiation and motion responses of the breakwater. Referring to Fig. 7, both the surge and heave RAOs are small at $W/L \approx 0.29$. The velocity due to the pitch motion is $\omega A_i RAO_{pitch} r$, where $r = 0.385$ m is the distance from the lower edge of the breakwater to the CG and the maximum pitch RAO is $RAO_{pitch} = 5.71$ at $W/L \approx 0.29$. If the velocity of wave motion (incident, scattered and radiated waves) is approximately equal to ωA_i (the actual velocity of wave motion at the lower edge of the breakwater should be smaller than ωA_i because of the dissipation and redistribution of incoming-wave energy), the ratio of the velocity due to the pitch motion to the velocity due to the wave motion (i.e. $\omega A_i RAO_{pitch} r / \omega A_i$) should be larger than 2.2, implying that the energy loss is controlled by the pitch motion of the floating breakwater at $W/L \approx 0.29$.

Referring to Figs. 5 and 6, the slotted barriers made the maximum energy loss and the minimum wave transmission occur at different values of W/L. At $W/L \approx 0.29$, the minimum transmission coefficient occurred, but the energy loss was not the maximum, suggesting that the transmission coefficient was affected by the interaction between the scattered waves and radiated waves. Obviously, the slotted barriers have altered the phase differences between the scattered waves and the radiated waves.

Referring to Figs. 6 and 7, the slotted barriers shifted the maximum energy-loss coefficient to $W/L \approx 0.26$. When the maximum energy loss occurred, the slotted barrier significantly reduced both the pitch and surge RAOs (the slightly-reduced heave RAOs might be due partly to the weakly coupling among the three RAOs); a reduction in the pitch RAOs may reduce the energy loss due to the vortex shedding at the sharp edges of the breakwater. Therefore, at $W/L \approx 0.26$, the energy loss increased by the slotted barriers is due mainly to the work done by the drag forces acting on the slotted barriers.

3.2 *Breakwater model with slotted barriers: effects of A_i/d*

Transmission and reflection coefficients

The reflection and transmission coefficients measured at various values of A_i/d are shown in Fig. 8 for three values of W/L: 0.292, 0.256 and 0.228. For $W/L = 0.292$, increasing A_i/d from 1.132 to 3.414 slightly decreased the reflection coefficient from 0.60 to 0.50; the transmission coefficient varied within the range of 0.04 and 0.11, and a minimum transmission coefficient of about 0.04 was obtained at $A_i/d = 1.753$. For $W/L = 0.256$, increasing A_i/d slightly decreased both the reflection and transmission coefficients. For $W/L = 0.228$, the reflection coefficients were not sensitive to A_i/d, but increasing A_i/d from 1.132 to 3.414 decreased the transmission coefficient from 0.75 to 0.57.

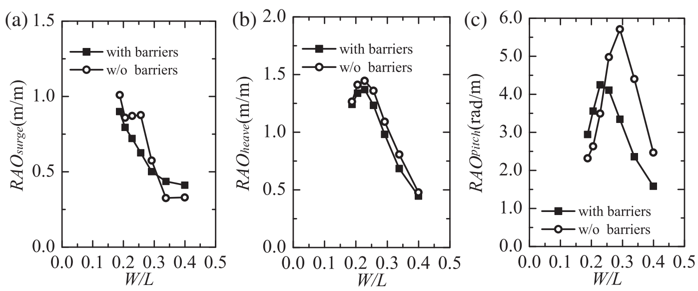

Figure 7 Effects of the slotted barriers on the measured RAOs: (a) surge RAOs, (b) heave RAOs and (c) pitch RAOs

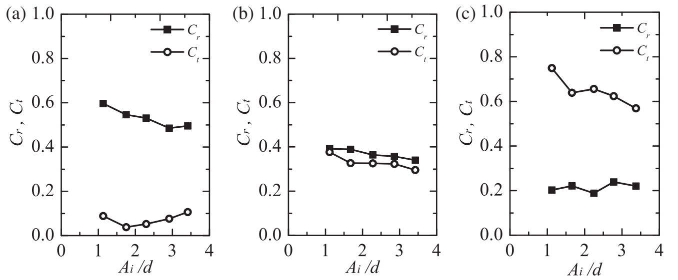

Figure 8 Reflection and transmission coefficients as functions of A_i/d for three values of W/L: (a) $W/L = 0.292$, (b) $W/L = 0.256$ and (c) $W/L = 0.228$

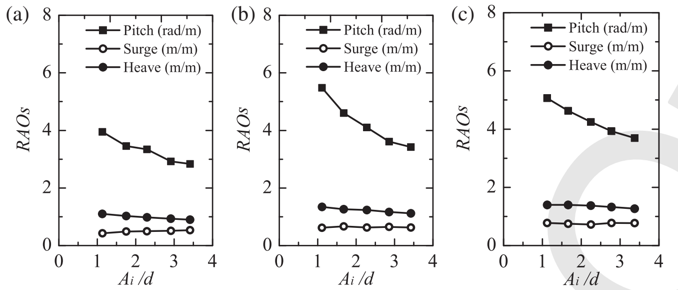

Figure 9 Pitch, surge and heave RAOs as functions of A_i/d for three values of W/L: (a) $W/L = 0.292$, (b) $W/L = 0.256$ and (c) $W/L = 0.228$

Huang (2007) has shown that for a fixed slotted barrier, increasing A_i/d with a fixed wave period tends to reduce the transmission coefficient and slightly increase the reflection coefficient. However, for the slotted barriers installed on a floating structure, the effects of A_i/d on wave transmission and reflection coefficients are not so obvious, possibly because that the surge response of the breakwater may reduce the relative velocity between the slotted barriers and the surrounding water.

Motion responses

The effects of A_i/d on motion responses are shown in Fig. 9. In general, both the surge and heave RAOs were not sensitive to A_i/d. However, the pitch RAOs decreased with increasing A_i/d for all three values of W/L. In particular, the pitch RAOs dropped from 5.5 to 3.4 rad m^{-1} when A_i/d was increased from 1.132 to 3.414 for W/L =0.256. The authors cannot provide a satisfactory explanation to the effects of A_i/d on the motion responses of the floating breakwater with slotted barriers, and a Q2 theory or CFD simulation may be needed to provide satisfactory physical explanations.

4 Conclusions

A comparative experimental study is reported to demonstrate the potential of using slotted barriers to improve the transmission performance of floating rectangular breakwaters. Experimental results showed that the slotted barriers attached to the bottom of a floating rectangular breakwater could significantly reduce the transmission coefficients, especially for longer waves. The slotted barriers significantly reduced the pitch responses for shorter waves but increased the pitch responses for longer waves; the slotted barriers also reduced the surge responses for longer waves, but increased the surge responses for shorter waves. The reduction of the heave responses by the slotted barriers was minor. For long waves, the reduction of transmission coefficients by the slotted barriers was related mainly to the increased energy loss associated with the enhanced pitch motion; for shorter waves, the reduction of transmission coefficients was related partly to the blockage effect by the slotted barriers. It is also argued that the slotted barriers are not likely to significantly increase the mooring-line force. The effects of steep regular waves, irregular waves, and the porosity and arrangement of slotted barriers are worth future investigation for optimum designs of such breakwaters.

Acknowledgements

The authors thank the Associate Editor and three anonymous reviewers for their constructive comments, which have greatly improved the quality of this paper.

Funding

DHI-NTU centre, Nanyang Technological University, Singapore, is acknowledged for its support to the third author. Nanyang Technological University is also acknowledged for its partial support to this work through grant SUG 03/07.

Notations

A_{heave}	=	amplitude of the heave response (m)
A_i	=	incident wave amplitude (m)
A_r	=	reflected wave amplitude (m)
A_{rb}	=	amplitude of wave reflected from absorbing beach (m)
A_{surge}	=	amplitude of the surge response (m)
A_t	=	transmitted wave amplitude (m)
$(A_x(t), A_z(t))$	=	translational accelerations in x- and z- direction measured by IMU (m s^{-2})
$(a_{x'}(t), a_{z'}(t))$	=	translational accelerations in x- and z- direction in the earth-fixed coordinate system (m s^{-2})
$(\hat{a}_{x'}, \hat{a}_{z'})$	=	amplitudes of translational accelerations in x- and z- direction in the earth-fixed coordinate system (m s^{-2})
C_l	=	energy-loss coefficient (–)
C_r	=	reflection coefficient (–)
C_{rb}	=	reflection coefficient of the absorbing beach (–)
C_t	=	transmission coefficient (–)
d	=	dimension of the cylinder (m)
h	=	water depth (m)
H_i	=	incident wave height (m)

KC = Keulegan–Carpenter number (–)
L = wave length (m)
R = Reynolds number (–)
r = the distance from the lower edge of the breakwater to the CG (m)
RAO_{heave} = heave RAO (–)
RAO_{pitch} = pitch RAO (rad m^{-1})
RAO_{surge} = surge RAO (–)
(r_x, r_z) = the coordinates of the CG in the IMU-fixed coordinate system (m)
T = wave period (s)
U = Ursell number (–)
U_m = velocity amplitude (m s^{-1})
W = width of the floating breakwater (m)
(x, z) = IMU-fixed coordinate system
(x', z') = earth-fixed coordinate system
$\dot{\theta}(t)$ = pitch angular-velocity measured by IMU (rad s^{-1})
$\hat{\dot{\theta}}$ = amplitude of the pitch angular-velocity (rad s^{-1})
$\ddot{\theta}(t)$ = pitch angular-acceleration (rad s^{-2})
v = kinematic viscosity (m^2 s^{-1})
$(\phi_{a_{x'}}, \phi_{a_{z'}})$ = initial phases of translational accelerations in x- and z- direction in the earth-fixed coordinate system (rad)
ω = wave angular frequency (rad s^{-1})

References

Aristodemo, F., Tomasicchio, G.R., Veltri, P. (2011). New model to determine forces at on-bottom slender pipelines. *Coastal Eng.* 58(3), 267–280.

Black, J.L., Mei, C.C., Bray, M.C.G. (1971). Radiation and scattering of water waves by rigid bodies. *J. Fluid Mech.* 46(1), 151–164.

Drimer, N., Agnon, Y., Stiassnie, M. (1992). A simplified analytical model for a floating breakwater in water of finite depth. *Appl. Ocean Res.* 14(1), 33–41.

Faltinsen, O.M. (1993). *Sea loads on ships and offshore structures*. Cambridge University Press, Cambridge, UK.

Goda, Y., Suzuki, Y. (1976). Estimation of incident and reflected waves in random wave experiments. Proc. 15th Int. Conf. *Coastal Engineering, ASCE*, Honolulu, HI, 828–845.

He, F., Huang, Z.H., Law, A.W.K. (2012). Hydrodynamic performance of a rectangular floating breakwater with and without pneumatic chambers: An experimental study. *Ocean Eng.* 51(0), 16–27.

He, F., Huang, Z.H., Law, A.W.K. (2013). An experimental study of a floating breakwater with asymmetric pneumatic chambers for wave energy extraction. *Appl. Energy* 106(0), 222–231.

Huang, Z.H. (2007). Wave interaction with one or two rows of closely spaced rectangular cylinders. *Ocean Eng.* 34(11/12), 1584–1591.

Huang, Z.H., Li, Y., Liu, Y. (2011). Hydraulic performance and wave loadings of perforated/slotted coastal structures: A review. *Ocean Eng.* 38(10), 1031–1053.

Koutandos, E., Prinos, P., Gironella, X. (2005). Floating breakwaters under regular and irregular wave forcing: Reflection and transmission characteristics. *J. Hydraulic Res.* 43(2), 174–188.

Le Mehaute, B. (1976). *An introduction to hydrodynamics and water waves*. Springer-Verlag, New York.

Mani, J.S. (1991). Design of Y-frame floating breakwater. *J. Waterw. Port Coast. Oc. Eng.* 117(2), 105–119.

Mavrakos, S.A. (1992). *STATMOOR user's manual*. Laboratory for Floating Structures and Mooring Systems, School of Naval Architecture and Marine Engineering, National Technical University of Athens, Athens, Greece.

McCartney, B.L. (1985). Floating breakwater design. *J. Waterw. Port Coast. Oc. Eng.* 111(2), 304–318.

Mei, C.C., Stiassnie, M., Yue, D.K.F. (2005). *Theory and applications of ocean surface waves—Part 1: Linear aspects*. World Scientific, Singapore.

Peña, E., Ferreras, J., Sanchez-Tembleque, F. (2011). Experimental study on wave transmission coefficient, mooring lines and module connector forces with different designs of floating breakwaters. *Ocean Eng.* 38(10), 1150–1160.

Ruol, P., Martinelli, L., Pezzutto, P. (2013). Formula to predict transmission for Π-type floating breakwaters. *J. Waterw. Port Coast. Oc. Eng.* 139(1), 1–8.

Sannasiraj, S.A., Sundar, V., Sundaravadivelu, R. (1998). Mooring forces and motion responses of pontoon-type floating breakwaters. *Ocean Eng.* 25(1), 27–48.

Sarpkaya, T., Isaacson, M. (1981). *Mechanics of wave forces on offshore structures*. Van Nostrand Reinhold Company, New York.

Sawaragi, T. (1995). *Coastal engineering: Waves, beaches, wave–structure interactions*. Elsevier, Amsterdam.

Tomasicchio, G.R., D'Alessandro, F. (2013). Wave energy transmission through and over low crested breakwaters. *J. Coast. Res.* SI 65(1), 398–403.

Vijayakrishna Rapaka, E., Natarajan, R., Neelamani, S. (2004). Experimental investigation on the dynamic response of a moored wave energy device under regular sea waves. *Ocean Eng.* 31(5–6), 725–743.

Wang, H.Y., Sun, Z.C. (2010). Experimental study of a porous floating breakwater. *Ocean Eng.* 37(5–6), 520–527.

Williams, K.J. (1988). An experimental study of wave–obstacle interaction in a two-dimensional domain. *J. Hydraulic Res.* 26(4), 463–482.